

## Numerical investigation of flow on NACA4412 aerofoil with different aspect ratios

Hacimurat Demir<sup>1,2,a</sup>, Mustafa Özden<sup>1</sup>, Mustafa Serdar Genç<sup>1</sup>, Mücahit Çağdaş<sup>1</sup>

<sup>1</sup>Wind Engineering and Aerodynamic Research Group, Department of Energy Systems Engineering, Erciyes University, Kayseri, Turkey

<sup>2</sup>Department of Mechanical Engineering, Aksaray University, Aksaray, Turkey

**Abstract.** In this study, the flow over NACA4412 was investigated both numerically and experimentally at a different Reynolds numbers. The experiments were carried out in a low speed wind tunnel with various angles of attack and different Reynolds numbers (25000 and 50000). Airfoil was manufactured using 3D printer with a various aspect ratios (AR = 1 and AR = 3). Smoke-wire and oil flow visualization methods were used to visualize the surface flow patterns. NACA4412 aerofoil was designed by using SOLIDWORKS. The structural grid of numerical model was constructed by ANSYS ICEM CFD meshing software. Furthermore, ANSYS FLUENT<sup>TM</sup> software was used to perform numerical calculations. The numerical results were compared with experimental results. Bubble formation was shown in CFD streamlines and smoke-wire experiments at  $z/c = 0.4$ . Furthermore, bubble shrunk at  $z/c = 0.2$  by reason of the effects of tip vortices in both numerical and experimental studies. Consequently, it was seen that there was a good agreement between numerical and experimental results.

### 1 Introduction

Low Reynolds (Re) number aerodynamics has gained more attention due to increasing applications of Micro Air Vehicle (MAV), Unmanned Air Vehicle (UAV) and wind turbine. At low Reynolds number flows, laminar separation bubble may cause negative effects, such as increasing on drag, decreasing on lift, reducing stability of the aircraft, vibration, and noise [1–7]. Wind turbine blades, unmanned air vehicles (UAV), micro air vehicles (MAV) and propellers are some examples of applications of low Reynolds number aerodynamics. In low Reynolds number flow regime, viscous forces are higher than inertia forces. The fluid flow is prone to separate, resulting in increases in drag and loss of efficiency under low Reynolds number regime.

Under such low Reynolds number regime, the maximum lift and stall angle are lower than high Reynolds number flow conditions. Due to the fact that the aerodynamic performance is lower, it is vital to control the flow and to achieve higher lift for this type of vehicles and devices. There are new methods being developed to ignore the negative effects of the separated flow for improving the aerodynamic performance. These methods called flow control methods and these methods could be categorized as active and passive [5–7]. Active flow control method can be made by adding energy to free stream or to boundary layer directly. On the other hand, passive flow control method can be executed by

adding geometrical discontinuities. The active flow control methods can be suction and/or blowing [6] or high lift devices [7], the passive control methods can be vortex generators [8] or flexibility enhancer [9–10]. Lift can be increased, drag force can be reduced, stall can be delayed, vibrations and noise can be diminished and reattachment of the separated flow can be ensured by means of utilizing these flow control methods.

A series of studies have been executed to understand and determine the low Reynolds number aerodynamics around entirely translating low-aspect-ratio wings. [11–14]. R. Wahidi et al. [15] investigated to effects of laminar separation bubbles by measuring over NACA4412 airfoil model using volumetric three-component velocimetry (V3V) and particle image velocimetry (PIV) at Reynolds number 50000 and different angle of attack. They defined that onset of transition, location of separation and reattachment after they made comment relationships of different Reynolds normal and shear stress via the time-averaged V3V. Their results demonstrated that roll-up of spanwise caused vortices and these vortices inspired pairs of negative and positive wall-normal velocity. The pairs did an enormous act in the uncertainty of the reattachment of the separated shear layer. M. Agrawal and G. Saxena [16] aimed that making analysis for aerodynamic of wings. They selected NACA4412 airfoil as a model and achieved few results after completing wind tunnel tests sections. They observed from results that lift increased until a certain

<sup>a</sup>Corresponding author: hmdemir@aksaray.edu.tr

point if angle of attack increased. Their observation also included that drag started to become a dominant factor if angle of attack kept rising and stall occurred as a result of all these parts.

Karasu et al. [17] performed a numerical study on low Reynolds number flow over NACA2415 airfoil and compared the numerical results with the experimental results of their previous study [4, 18]. It was stated that the point of separation moved towards the leading edge due to increasing angle of attack. Moreover, the flow visualization results showed that as the angle of attack increased further, the bubble burst and the separated flow was not able to reattach to the airfoil surface, which indicated stall. Furthermore, in the numerical results, the transition models are shown to definitely predict the location of the separation bubble experimentally determined at lower angles of attack.

## 2 Numerical Modelling of Airfoil

For numerical model, manufacturing of NACA4412 airfoils with different aspect ratios were conducted by using SOLIDWORKS software. ANSYS Workbench module was utilized for numerical modelling of flow over the airfoil. The grid structures of test section and airfoil surface were constructed by means of ICEM CFD. The domain except the airfoil was selected as pressure far field and no slip condition was carried out to the airfoil surface. All calculations were performed on as density based, and steady-state solution.

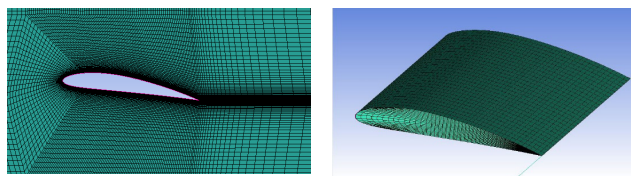


**Figure 1.** The detailed view of the mesh NACA4412 aerofoil.

ANSYS Fluent software was used for calculation and SST Transition model was used for the numerical solution method.

### 2.1 Experimental Study

#### 2.1.1 Experimental apparatus and methods

The experiments were carried out in a low-speed, suction-type wind tunnel with a square working section of 500 mm x 500 mm located at the Department of Energy Systems Engineering, University of Erciyes via Wind Engineering and Aerodynamics Research Group (WEAR) as shown in Figure 2. Turbulence intensity of the tunnel is 0.35% and the operating range of tunnel speed was 1-45 m / s. The experiments were conducted at Reynolds numbers (Re) of 25000 and 50000.

NACA4412 airfoil was manufactured by means of 3D printer as seen in Figure 3.



**Figure 2.** Photograph of the experimental set-up.

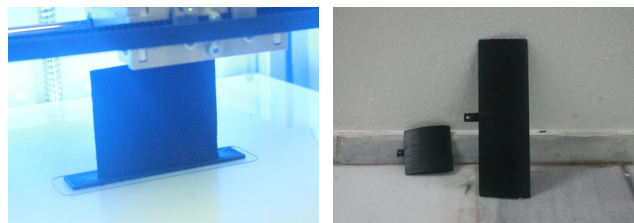


**Figure 3.** NACA4412 airfoils with different aspect ratios.

#### 2.1.2 Smoke-wire and oil flow visualization

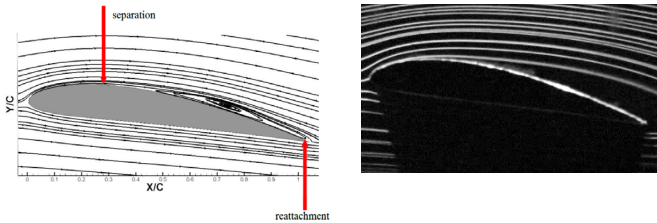
The smoke-wire technique allows for the introduction of fine smoke streamlines into the flow field through the electrical resistive heating of a very thin wire which has been coated with oil and which is located upstream from the leading edge of the related airfoil section. Smoke-wire tests have been conducted to visualize flows over NACA4412 airfoil surface at  $z/c = 0.2$  and  $z/c = 0.4$  and two different Reynolds numbers ( $Re = 25000$  and  $Re = 50000$ ) with various aspect ratios ( $AR = 1$  and  $AR = 3$ ) at  $8^\circ$  angle of attack. The expression of  $z/c$  is utilized for the location of smoke wire.

Oil flow visualization technique was employed for the flow visualization because this technique was simple like smoke-wire method to apply and effective to see flow conditions. In order to photograph the surface flow events using this method, the pigmented oils are painted onto NACA4412 airfoil surface (Figure 7). Once it has dried, the painted and patterned surface can be photographed. The mix should have the right consistency to efficaciously demonstrate boundary layer development. Additionally, the inertia forces of the moving oil should be lower than the viscous and surface tension forces [19] to not affect the conditions at the surface. Kerosene, light diesel oil and light transformer oil are most common oils, and titanium dioxide, china clay and fluorescent chrysene are most common pigments [19]. In addition to this, oleic acid can be added to the mixture to clearly see the pigment deposit on the oiled surface. The simplest mix to make was kerosene, titanium dioxide and a very small amount of oleic acid: the ratio of kerosene to oleic acid was roughly 20:1 [20] and this ratio of mixture was utilized in the present study.

### 3 Comparisons between Experimental and Numerical Results

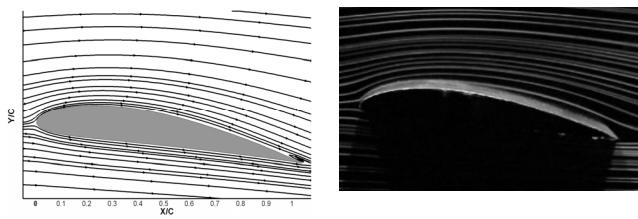
#### 3.1 Effects of tip vortex on separation bubble

When obtained experimental and numerical results are analyzed, bubble formation is observed in streamline and smoke-wire at  $z / c = 0.4$ . Furthermore, bubble shrunk at  $z / c = 0.2$  due to the effects of tip vortices. The effects of tip vortices could be understood significantly with oil experiment.



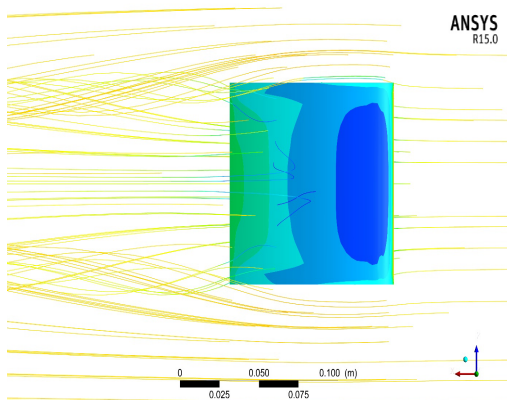
(a) Numerical stream lines on the NACA 4412 (b) Experimental smoke-wire visualization result

Figure 4. NACA4412 airfoil results for  $Re = 25000$ ,  $AR = 3$  and  $z / c = +0.4$  condition.

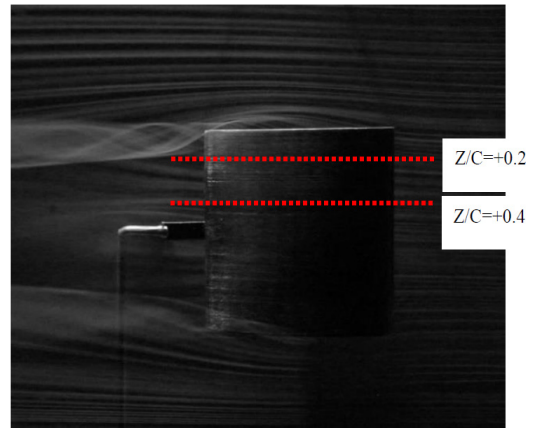


(a) Numerical stream lines on the NACA4412 (b) Experimental smoke-wire visualization result

Figure 5. NACA4412 airfoil results for  $Re = 25000$ ,  $AR = 3$  and  $z / c = +0.2$  condition.



(a) Numerical stream lines on the NACA 4412.

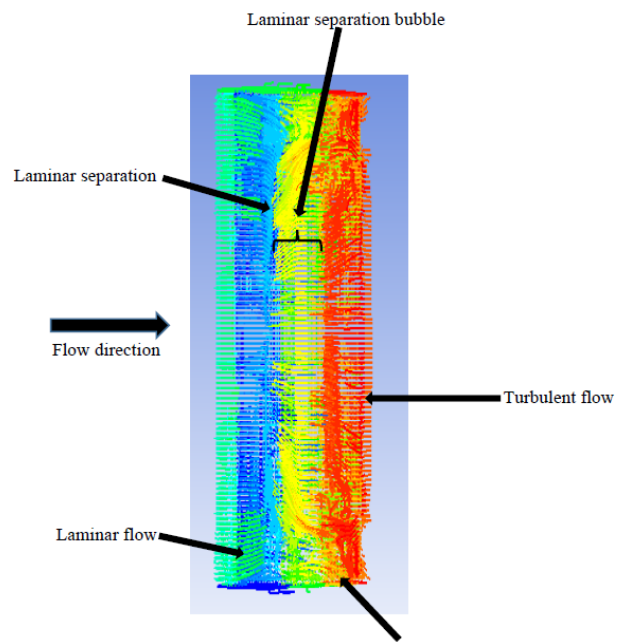


(b) Experimental smoke-wire visualization result.

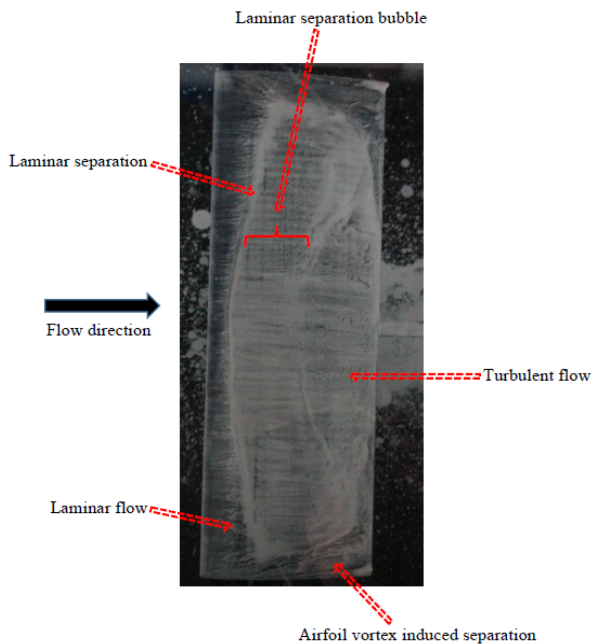
Figure 6. Tip vortices at  $z / c = +0.4$  and  $Re = 50000$  for  $AR = 1$  airfoil.

It is seen that tip vortices have an impact on the inner of the airfoil when comparing the smoke wire experimental and numerical results. It is observed that flow moved from lower side to the upper side of the airfoil due to the pressure side.

The effects of separation over the airfoil are seen after obtained oil flow visualization results. There is no change of oil mixture over the airfoil where flow separation is occurred but oil is swept at the location of the flow which is attached to the airfoil. When moving to the  $z$  direction on the airfoil, the size of separation increases in the middle location of the airfoil. On the other hand, oil mixture moves to inside of airfoil in the tip region. Tip vortices which are occurred on the airfoil tip affect the flow over the airfoil significantly. Furthermore, leading edge vortices combine with tip vortices and this situation causes to ensure 3D vortices. Flow obtains energy and bubble decreases due to these 3D vortices.



(a) Numerical result, upper side



(b) Experimental oil flow visualization results, upper side

**Figure 7.** Numerical and experimental results for  $Re = 50000$  and  $AR = 3$ .

## 4 Conclusion

In this study, the flow over NACA4412 airfoil which was manufactured by means of 3-D printer with  $AR = 1$  and  $AR = 3$  was investigated both numerically and experimentally at various Reynolds numbers. The experimental section was conducted in a low speed wind tunnel with various angles of attack and  $Re = 25000$  and  $Re = 50000$ . In order to visualize the surface flow patterns of NACA4412 smoke-wire and oil flow visualization methods were utilized. Furthermore, the structural grid of numerical model was constructed by ANSYS ICEM CFD meshing software. Additionally, ANSYS FLUENT™ software was used to perform numerical calculations. The numerical results were compared with experimental results and it was seen that bubble formation occurred in streamline and smoke-wire at  $z/c = 0.4$ . In addition to this, by reason of the effects of tip vortices bubble shrunk at  $z/c = 0.2$ .

The effects of tip vortices could be understood significantly with oil experiment. There was no change of oil mixture over the airfoil where flow separation was occurred but oil was swept at the location of the flow which was attached to the airfoil. In the tip region, oil mixture moved to inside of airfoil. Tip vortices which were occurred on the airfoil tip affected the flow over the airfoil importantly. Additionally, leading edge vortices combined with tip vortices and this situation caused to ensure 3D vortices. Flow obtained energy and bubble decreased due to these 3D vortices. It was seen from the obtained results that there was a good agreement between numerical and experimental results.

## Acknowledgments

The authors would like to acknowledge funding from the Scientific and Technological Research Council of Turkey (TÜBİTAK) under the project no: 213M329.

## References

1. W. Zhang, R. Hain, C.J. Kahler, Scanning PIV investigation of the laminar separation bubble on a SD7003 airfoil. *Exp. Fluids*. **45(4)**, 725-743 (2008)
2. R. Ricci, S.A. Montelpare, Quantitative IR thermographic method to study the laminar separation bubble phenomenon. *Int J Therm Sci*. **44(8)**, 709-719 (2005)
3. M.S. Genc, Numerical Simulation of Flow over a Thin Aerofoil at High Re Number using a Transition Model. *Proc IMechE, Part C-J Mech Eng Sci*, **224(10)**, 2155-2164 (2010)
4. M.S. Genc, I. Karasu, H.H. Acikel, An experimental study on aerodynamics of NACA2415 aerofoil at low Re numbers. *Exp Therm Fluid Sci*. **39**, 252-264 (2012)
5. M.S. Genc, I. Karasu, H.H. Acikel, M.T. Akpolat, Low Reynolds number flows and transition, in: M. Serdar Genc (Ed.), *Low Reynolds Number Aerodynamics and Transition*, *Intech-Sciyo Publishing*, ISBN 979-953-307-627-9 (2012)
6. M.S. Genc, U. Kaynak, H. Yapıcı, Performance of transition model for predicting low Re aerofoil flows without/with single and simultaneous blowing and suction. *Eur J Mech B-Fluid*. **30(2)**, 218-235 (2011)
7. M.S. Genc, U. Kaynak, G.D. Lock, Flow over an Aerofoil without and with Leading Edge Slat at a Transitional Reynolds Number. *Proc IMechE, Part G: J Aerospace Eng*. **223(3)**, 217-231 (2009)
8. D. Lengani, D. Simoni, M. Ubaldi, P. Zunino, F. Bertini, Turbulent boundary layer separation control and loss evaluation of low profile vortex generators. *Exp Therm Fluid Sci*. **35(8)**, 1505-1513 (2011)
9. M.S. Genç, Unsteady aerodynamics and flow-induced vibrations of a low aspect ratio rectangular membrane wing with excess length. *Exp. Therm Fluid Sci*. **44**, 749-759 (2013)
10. P. Rojratsirikul, M.S. Genc, Z. Wang, I. Gursul, Flow-induced vibrations of low aspect ratio rectangular membrane wings. *J Fluid Struct*. **27**, 1296-1309 (2011)
11. G.E. Torres, T.J. Mueller, Low aspect ratio aerodynamics at low Reynolds numbers. *AIAA journal*. **42(5)**, 865-873 (2004)
12. A. Pelletier, T.J. Mueller, Low Reynolds number aerodynamics of low-aspect-ratio, thin/flat/cambered-plate wings. *J Aircraft*. **37(5)**, 825-832 (2000)
13. P. Freymuth, W. Bank, F. Finaish, Further visualization of combined wing tip and starting vortex systems. *AIAA journal*. **25(9)**, 1153-1159 (1987)
14. P.H. Cosyn, J. Vierendeels. Numerical investigation of low-aspect-ratio wings at low Reynolds numbers. *J Aircraft*. **43(3)**, 713-722 (2006)

15. R. Wahidi, W. Lai, J.P. Hubner, A. Lang. Volumetric three-component velocimetry and PIV measurements of Laminar Separation Bubbles on a NACA4412 Airfoil. *16th Int. Symp of Applications of Laser Techniques of Fluid Mechanics*. Lisbon, Portugal. 09-12 July, (2012)
16. M. Agrawal, G. Saxena, Analysis of wings using airfoil NACA4412 at different angle of attack. *IJMERA*. **3**, 1467-1469 (2013)
17. I. Karasu, M.S. Genç, H.H. Açikel, Numerical study on low Reynolds number flows over an Aerofoil. *J. Appl. Mech. Eng.* **2**, 131 (2013)
18. I. Karasu, Experimental and numerical investigations of transition to turbulence and laminar separation bubble over aerofoil at low Reynolds number flows. Graduate School of Natural and Applied Sciences, Erciyes University, Kayseri, Turkey (2011)
19. Werzkirch, Flow Visualization, Academic Press Inc. Ltd., London, (1974)
20. D.F. Perrens, Flow visualisation in low speed wind tunnels. *Phys. Educ.* **5** (5), 262-265 (1970)